Ultrafast response of ErAs islands in GaAs

C. Kadow[1], J.P. Ibbetson[2], S.B. Fleischer[2], A.C. Gossard[1,2], J.E. Bowers[2]

[1]*Materials Department, UCSB, Santa Barbara, CA 93106*
[2]*Department of Electrical and Computer Engineering, UCSB, Santa Barbara, CA 93106*
E-mail: kadow@engineering.ucsb.edu

Abstract: ErAs islands in GaAs were grown by molecular beam epitaxy. The carrier dynamics were investigated by time resolved differential reflection measurements. The dynamics are strongly dependent on the microstructure, and decay times as short as 200 fs were observed.

OCIS codes: (320.7100) Ultrafast measurements; (320.7130) Ultrafast processes in condensed matter, including semiconductors (160.5690) Rare earth doped materials; (160.6000) Semiconductors, including MQW

Introduction

Materials with ultrafast optical response allow photodetector operation at frequencies up to 560 GHz [1], [2] and fabrication of sources of THz radiation such as photomixers [3]. The most widely used material for these types of applications is low temperature grown GaAs (LTG-GaAs). It is well known that doping of semiconductors with transition or rare earth metals can yield fast nonradiative recombination times. In particular response times as short as 1.5 ps have been reported for Er-doped GaAs [4]. This paper reports on the first ultrafast measurements on a novel material consisting of ErAs islands in GaAs.

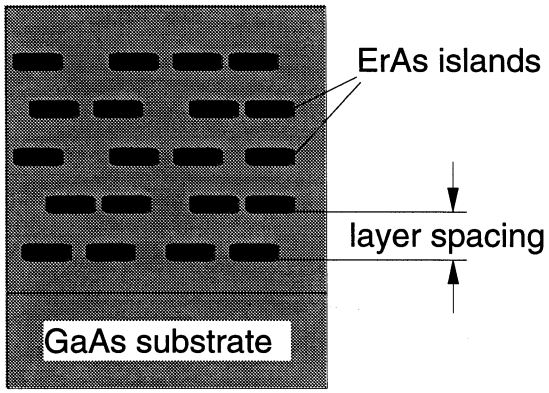

Figure 1: Schematic sample structure.

Growth and microstructure

The structure of the samples is outlined schematically in Figure 1. All samples are superlattices; they consist of equidistant layers of ErAs islands in a GaAs matrix. The material was grown on semi-insulating (100) GaAs substrates by molecular beam epitaxy (MBE) using a Varian Gen II solid source MBE machine. The GaAs was grown under standard growth conditions. The ErAs was grown at the same temperature of 535^{0}C as the GaAs matrix; the ErAs growth rate was

typically 0.04 monolayers (ML)/sec. The growth of ErAs occurs in Volmer-Weber growth mode resulting in island formation for an ErAs coverage of less than approximately 3 ML. For larger depositions the islands coalesce and films are formed [5]. It is possible to overgrow the ErAs islands with GaAs of high quality, and complete recovery of the RHEED pattern is observed after a few nm of overgrowth.

The high quality of the samples is also evident in the results of double crystal X-ray diffraction (DCXD) shown in Figure 2. Superlattice fringes can clearly be seen in the data. The superlattice period calculated from these fringes agrees within 2 % with the design. The splitting between the GaAs substrate peak and the zeroth order superlattice peak indicates compressive strain in the superlattice. This is expected because the ErAs lattice constant exceeds the GaAs lattice constant by 1.6 %.

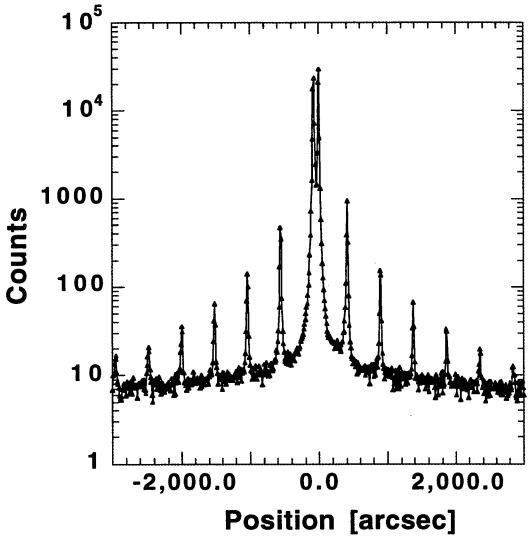

Figure 2: X-ray rocking curve.

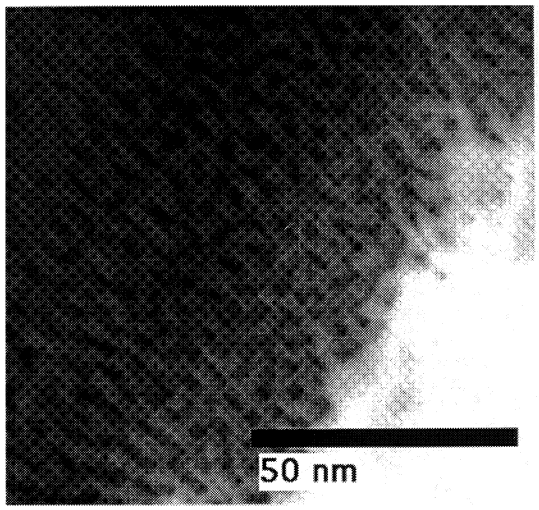

Figure 3: Plan-view TEM.

Figure 3 shows a plan view TEM of one of the samples studied (T_{growth} = 535^{0}C, 1.2 ML ErAs). From the TEM we estimate an island density of 7x10^{12} cm^{-2} and a diameter between 1 nm and 2 nm. The density and size of the islands can be controlled to some extent by the growth parameters. A higher growth temperature leads to larger islands and a higher ErAs-deposition results in a higher density of the islands. The exact dependences are currently under investigation.

The high level of control over the position in the growth direction, size and density of the particles allows us to study the influence of these parameters on the properties of the samples and should allow engineering the properties of the material. Since the islands are not formed by precipitation, the material is stable up to temperatures of 700^{0}C, allowing standard III-V processing.

Ultrafast measurements

Time resolved differential reflectance measurements are performed on samples grown under different growth conditions. The experimental setup is a pump-probe arrangement using short laser pulses generated by a mode-locked Ti:sapphire laser. The laser pulses are centered at wavelengths ranging from 800 nm to 860 nm. They are between 80 fs and 200 fs long. The pump and the probe pulses are polarized orthogonally to each other. The pump beam is modulated with an acousto-optical modulator at 9.0 MHz. Additionally the pump and the probe beam are modulated with a mechanical chopper at 2.5 kHz and 2.0 kHz respectively. The average powers are typically 10 mW for the pump beam and 350 μW for the probe beam. The signal is measured using lock-in detection. The dependence of the ΔR/R-signals on the probe power has been measured on several samples. It is found that the signals are independent of probe power for the power levels used. The spot size on the sample is about 50 μm as measured with pinholes placed at the sample position. This agrees well with the spot size expected from lens and beam parameters. We estimate that each pump pulse generates approximately $5x10^{17}$ cm^{-3} carriers when absorbed in GaAs. All wavelengths used are shorter than the wavelength corresponding to the GaAs band gap of 870 nm at room temperature.

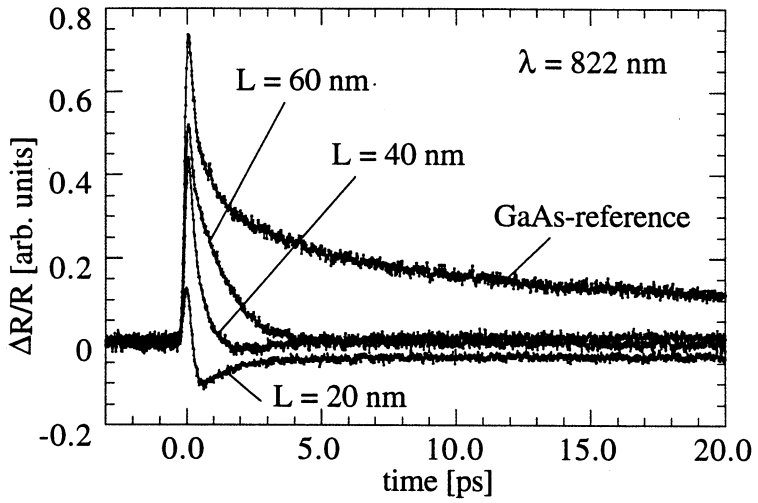

Figure 4: Time resolved differential reflectance for several samples.

Figure 4 compares results from three samples that contain ErAs-islands with a GaAs reference sample. The GaAs reference sample is a 1 μm thick GaAs film on a GaAs substrate grown under the same conditions as the ErAs containing films. The ErAs containing samples differ from each other by the period of the superlattice L (L = 20 nm, L = 40 nm and L = 60 nm). The three samples have the following structures: 20 x (0.6 ML ErAs, 60 nm GaAs), 40 x (0.6 ML ErAs, 40 nm GaAs), 60 x (0.6 ML ErAs, 20 nm GaAs).

The data shows that first, having the ErAs-islands changes the observed signal significantly: After an initial positive transient the signal returns to a value close to the baseline within a few picoseconds in contrast to the GaAs-reference. Second, the different periods L of

the superlattice structures change both the magnitude and the decay time of this initial transient response seen in all three ErAs containing samples. Third, some of the recorded ΔR/R-traces contain additional features besides the initial transient response; for example the sample with the 20 nm period in Figure 4 contains an additional negative term.

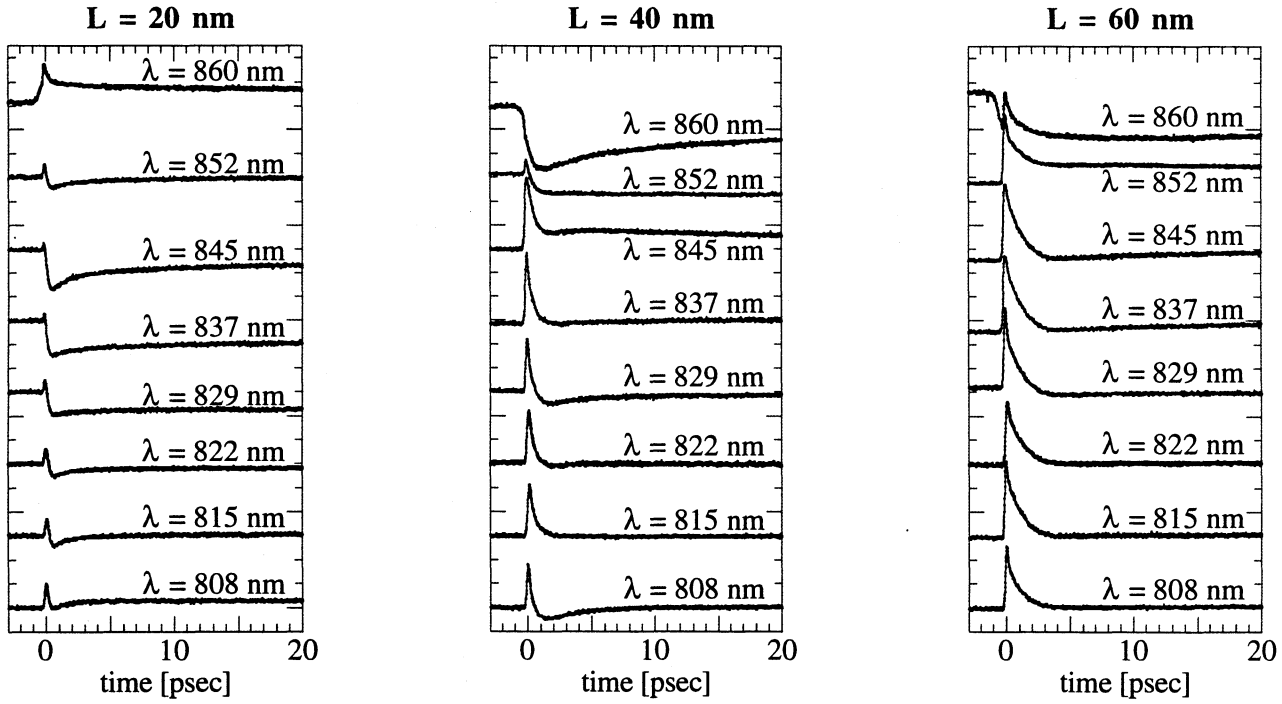

Figure 5: Spectral dependence of the time resolved differential reflectance for samples with superlattice periods L of L = 20 nm, L = 40 nm and L = 60 nm.

Figure 5 shows the spectral dependence of the time resolved differential reflectance for the same samples shown in Figure 4. It can be seen that the positive initial transient is the dominant contribution to the signal for the samples with L = 60 nm and L = 40 nm for wavelength shorter than approximately 850 nm. A similar initial decay is also seen in the sample with a period of L = 20 nm. It is however spoiled in many cases by an additional negative term. The time constant τ_1 associated with the initial decay shows hardly any dependence on the wavelength. τ_1 does depend strongly on the period L of the superlattice; τ_1 increases monotonically with L. The data in Figure 5 also shows that many ΔR/R-traces contain an additional negative transient. This term is most clearly seen in the sample with L = 20 nm and in some cases is the dominant contribution to the signal. The magnitude and the associated time constant of this feature have a strong spectral dependence. This term can also be seen in the sample with L = 40 nm, especially at wavelengths of λ = 808 nm and λ = 829 nm.

The data in Figure 5 is fit with either a single exponential function or the sum of two exponential terms to obtain numbers for the different time constants. Figure 6 shows the time constant τ_1 for the initial decay obtained from such fits as a function of the superlattice period L. τ_1 increases in a superlinear fashion with L. Figure 6 also includes a quadratic fit to the data. A fit

with this functional form may overinterpret the data especially since it has not been deconvoluted with the pulse shape. If the functional form is correct, it is consistent with a diffusion process and yields a diffusion constant of $D = 36\ cm^2\ sec^{-1}$. The time constant τ_1 is also found to be insensitive to how much ErAs is deposited in each layer of the superlattice.

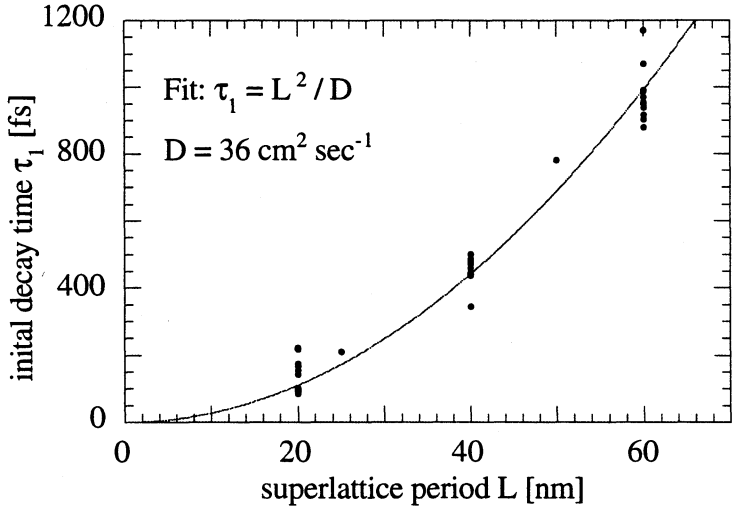

Figure 6: Initial decay time τ_1 as a function of the superlattice period L.

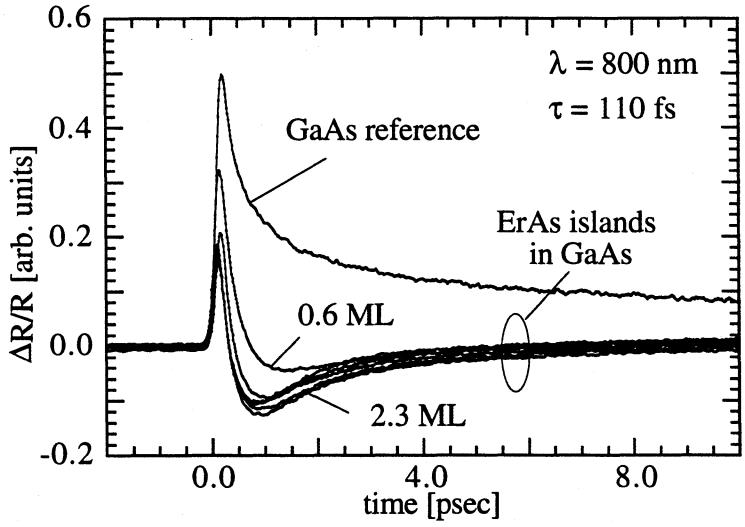

Figure 7: Time resolved differential reflectance DR/R for samples with different ErAs-deposition Y in each layer of the superlattice (Y = 0.6 ML, 1.2 ML, 1.5 ML, 1.8 ML, 2.0 ML, 2.3 ML).

Figure 7 shows data for samples with different ErAs deposition Y in each layer of the superlattice. The samples have the following structures 10x(Y ErAs, 25 nm GaAs) with Y = 0.6 ML, 1.2 ML, 1.5 ML, 1.8 ML, 2.0 ML, 2.3 ML. The time constant τ_1 of the initial decay has a value of approximately 230 fs independent of the ErAs deposition. When the amount of ErAs deposited in each layer is increased, the time constant of the second decay τ_2 decreases and the magnitude of this term increases. The time constant τ_2 ranges from 2.5 ps to 1.4 ps for samples with ErAs deposition between 0.6 ML and 2.3 ML respectively.

Discussion

The measured results are affected by the ErAs and the GaAs. The GaAs response is well understood and results from several processes. During the first ps the carrier distribution may be non-thermal. Afterwards the distribution is thermal and the signal is dominated by cooling of hot carriers to the bandedges and recombination [6].

We believe that the curves for the ErAs containing samples show some of these characteristics initially. Then, after a few 100 fs, the carriers created in the GaAs matrix are captured by the ErAs islands. We believe this to be the origin of the initial transient decay. A longer superlattice period L will lead to a longer time constant τ_1 because the carriers need more time to reach the ErAs islands. The quadratic fit in Figure 6 seems to indicate a diffusion process with diffusion constant D = 36 cm^2 sec^{-1}, which seems feasible for carriers in GaAs. However the time scale involved is so short that diffusion alone is too simple for an accurate description, and it is not clear that the carriers have thermalized.

Currently we do not understand the additional features seen in some traces at longer delay times. We speculate that they are linked to the relaxation within the ErAs islands.

Conclusions

We have reported the first ultrafast measurements on a novel material consisting of ErAs islands in GaAs. The growth of this material by MBE allows control of important parameters of the microstructure. Time resolved differential reflectance measurements show that the microstructure affects the rich carrier dynamics on a picosecond time scale significantly. In particular the superlattice period L determines the decay time τ_1 of the initial transient response, which can be as short as 200 fs. This observation is explained by capturing of carriers excited in the GaAs matrix by the ErAs-islands. The data contains additional features, which are currently not understood. We believe that this material is very promising for ultrafast applications such as THz-photomixers and ultrafast photodetectors.

Acknowledgements

We would like to acknowledge the support by Jet Propulsion Laboratory and the Center for Quantized Electronic Structures.

References

[1] Y.-J. Chiu, S.B. Fleischer, J.E. Bowers, IEEE Photonics Technology Letters **10**, 1012 (1998).

[2] P. Kordos, A. Förster, M. Marso, and F. Rüders, Electron. Lett. **34**, 119 (1998).

[3] E.R. Brown, K.A. McIntosh, K.B. Nichols, M.J. Manfra, and C.L. Dennis, Proceedings of the SPIE, vol. **2145**, 200 (1994).

[4] S. Gupta, S. Sethi, and P.K. Bhattacharya, Appl. Phys. Lett **62**, 1128 (1993).

[5] For a review on growth of rare earth arsenides see for example: T. Sands, C.J. Palmstrom, J.P. Harbison, V.G. Keramidas, N. Tabatabie, T.L. Cheeks, R. Ramesh, and Y. Silverberg, Mat. Sci. Rpts. **5 (3)**, 99 (1990).

[6] See for example: J. Shah, Ultrafast Spectroscopy of Semiconductors and Semiconductor Nanostructures, (Springer-Verlag, Berlin, 1996).